## Liquid Crystals

Publication details, including instructions for authors and subscription information:
http://www.informaworld.com/smpp/title~content=t713926090

# Banana-shaped mesogens: mesomorphic properties of seven-ring esters derived from 5-chlororesorcinol

S. Umadevi[a]; B. K. Sadashiva[a]
[a] Raman Research Institute, Sadashivanagar, Bangalore-560 080, India

**To cite this Article** Umadevi, S. and Sadashiva, B. K.(2005) 'Banana-shaped mesogens: mesomorphic properties of seven-ring esters derived from 5-chlororesorcinol', Liquid Crystals, 32: 3, 287 — 297

**To link to this Article: DOI:** 10.1080/02678290500031814

**URL:** http://dx.doi.org/10.1080/02678290500031814

*Liquid Crystals*, Vol. 32, No. 3, March 2005, 287–297

# Banana-shaped mesogens: mesomorphic properties of seven-ring esters derived from 5-chlororesorcinol

S. UMADEVI and B. K. SADASHIVA*

Raman Research Institute, C. V. Raman Avenue, Sadashivanagar, Bangalore-560 080, India

(*Received 16 September 2004; accepted 29 October 2004*)

Two new homologous series of seven-ring bent-core compounds derived from 5-chlororesorcinol have been synthesized. Many of the lower homologues in both series exhibit the rectangular columnar $B_1$ phase. However, the three analogous compounds having long terminal alkyl chains exhibit a switchable lamellar phase, which is different from the usual $B_2$ phase. Although the ground state structure of the mesophase is antiferroelectric, it shows chiral conglomerates with opposite tilt and polarity. Simultaneously, racemic structures are also seen. The mesophases have been characterized using a combination of polarized light microscopy, X-ray diffraction and electro-optical studies.

## 1. Introduction

The mesomorphic properties of compounds composed of banana-shaped or bent-core (BC) molecules have been investigated quite extensively [1–3]. Although the relationship between the chemical nature of a particular BC compound and the mesophase/s it exhibits is still not very clear, certain features have emerged which appear to be general along a homologous series of compounds. For example, the sequence of mesophases that appear on ascending a homologous series is intercalated smectic ($B_6$), a rectangular columnar ($B_1$) and a polar smectic ($B_2$) phase, which have been observed in many series of compounds [4, 5]. In most cases, the polar smectic phases show antiferroelectric characteristics. However, ferroelectrically switchable banana phases have been observed in several different compounds composed of specially designed molecules [6–10]. Amongst all the mesophases exhibited by BC compounds, the $B_7$ mesophase shows the most beautiful optical textures. One such characteristic texture of this phase is the growth of spiral germs on slow cooling of the isotropic phase. This phase could not be switched electro-optically and low resolution X-ray diffraction (XRD) data was insufficient to determine structure of the mesophase. Based on the nomenclature proposed [3] for this mesophase (which was first observed in compounds derived from 2-nitroresorcinol), there are a few reports in which similar optical textures and XRD data have been obtained for compounds containing a cyano group in the angular position and assigned the symbol $B_7$ [11–14].†

Interestingly, the growth of spiral domains has been observed in a number of other compounds which contain no substituent in the angular position of the central phenyl unit [6, 7, 15–17]. The mesophases exhibited by some of these compounds do switch electro-optically and the symbol $B_7$ has been assigned to them. Recently, the structure of the homochiral ferroelectric phases that show several different optical textures has been identified as a separate class of $B_7$ phase, using a combination of high resolution XRD, freeze fracture transmission electron microscopy, and depolarized transmission and reflection light microscopy [18]. The authors proposed that this $B_7$ phase has a polarization-modulated/undulated layer stripe structure.

Very recently, we reported the mesomorphic properties of several seven-ring achiral bent-core compounds derived from 5-cyanoresorcinol, and belonging to two homologous series [19]. The lamellar phase obtained for the higher homologues of both the series of compounds show a mixture of four different possible structures. Of these, two are chiral conglomerates with opposite tilt and polarity, and the remaining two have racemic structures. In addition, they exhibit helical and filamentary textures when observed under a polarizing microscope. Hence, this phase is different from the $B_2$ phase observed in a large number of compounds and has been

---

*Corresponding author. Email: sadashiv@rri.res.in

†Nomenclature $B_1$–$B_7$ was suggested at the workshop on banana-shaped liquid crystals: *Chirality by Achiral Molecules*, held in Berlin in December 1997.

*Liquid Crystals*
ISSN 0267-8292 print/ISSN 1366-5855 online © 2005 Taylor & Francis Group Ltd
http://www.tandf.co.uk/journals
DOI: 10.1080/02678290500031814

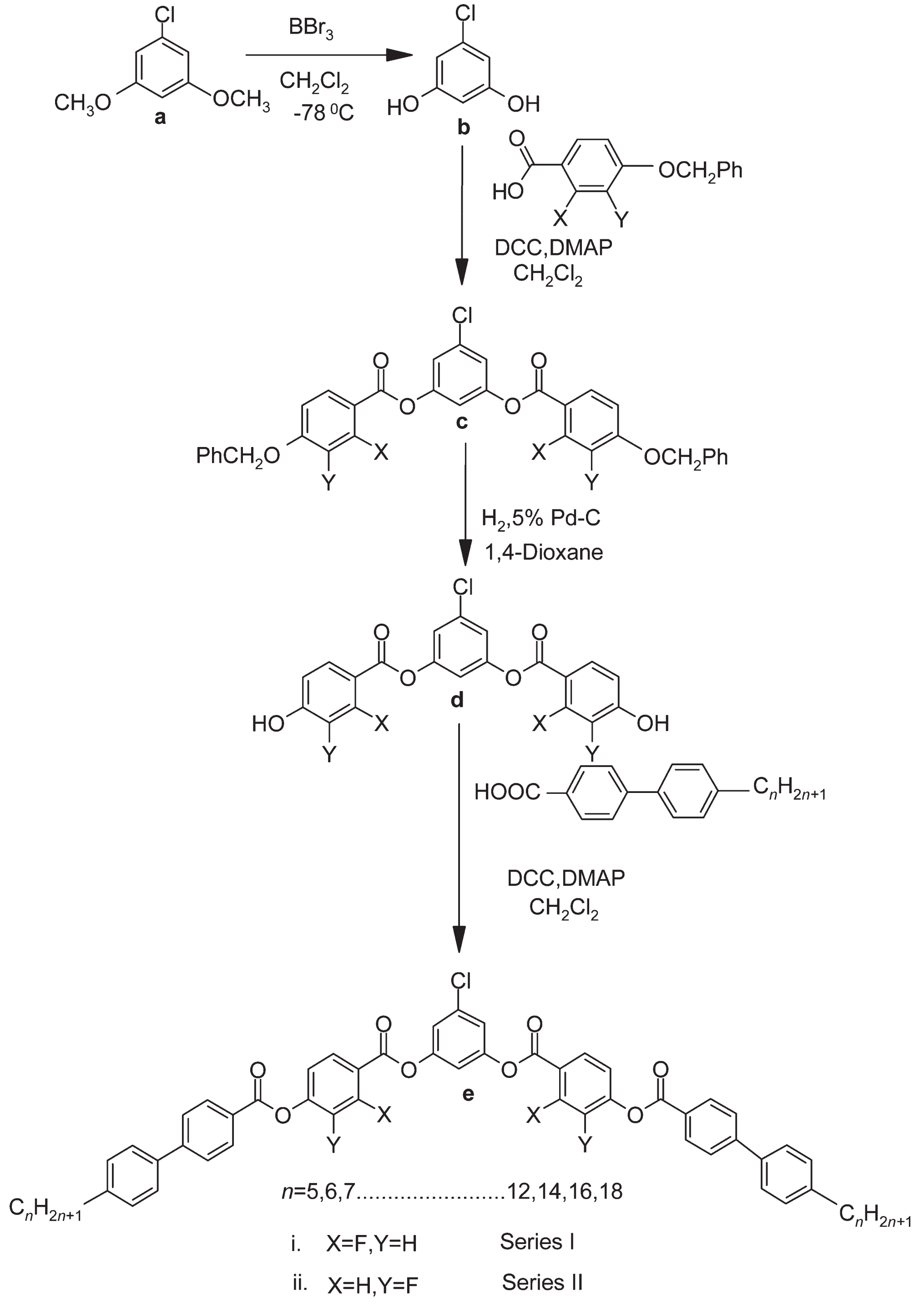

Scheme. Synthetic pathway used for the preparation of bent-core compounds.

designated the $B_{2x}$ phase. Here, we report the synthesis and characterization of analogous seven-ring bent-core compounds (structure **e** in the scheme) derived from 5-chlororesorcinol and belonging to two homologous series. The motivation for carrying out this investigation was to examine the effect of replacing the strongly polar cyano substituent (with the dipole moment along the arrow axis of the BC molecule) by a chloro group with a weaker dipolar component, but whose contribution is along the same axis. The synthesis of the investigated compounds was carried out following the pathway shown in the scheme.

## 2. Experimental

### 2.1. *Measurements*

The intermediate and target compounds were purified by column chromatography on silica gel (ACME, 60–120 mesh) and repeated crystallization from analytical grade solvents. Merck Kieselgel $60F_{254}$ precoated thin layer chromatographic plates were used to check the purity of the samples. The chemical structure of the compounds were determined by IR (Shimadzu FTIR-8400 spectrophotometer), $^1$H NMR (Bruker AMX 400 spectrometer), and elemental analysis (Carlo-Erba 1106 analyser).

The transition temperatures and associated enthalpies were determined by differential scanning calorimetry (DSC) (Perkin-Elmer, Model Pyris 1D), with calibration by indium as standard. The mesophase behaviour was studied using a polarising optical microscope (POM) (Leitz Laborlux 12 POL/Olympus BX 50) equipped with a heating stage and a central processor (Mettler FP 82HT and FP 90, respectively). XRD studies were carried out on unoriented powder samples taken in Lindemann capillaries of 0.7 mm diameter. $\mathrm{CuK}_\alpha$ (1.54 Å) radiation from a 4 kW rotating anode X-ray source (Rigaku Ultrax-18) with a graphite crystal monochromator was used. The diffraction patterns of the samples were collected on an image plate (Marresearch).

Polarization measurements were carried out using polyimide-coated ITO glass cells employing the triangular wave method. The triangular wave was generated by a waveform generator (Wavetek, Model 39) connected to a Trek Model 601B-3 amplifier. The current was measured across a 10 kΩ resistor and the current response traces were recorded using an Agilent Oscilloscope (54621A). The d.c. field experiments were carried out using a regulated dual d.c. power supply (APLAB, Model LD6401).

### 2.2. *Synthesis*

5-Chlororesorcinol was prepared from commercial 1-chloro-3,5-dimethoxybenzene as described below. 2-Fluoro-4-hydroxybenzoic acid and 3-fluoro-4-hydroxybenzoic acid were synthesized from 2-fluoroanisole and 3-fluoroanisole, respectively, following a procedure described in the literature [20]. 2-Fluoro-4-benzyloxybenzoic acid and 3-fluoro-4-benzyloxybenzoic acid were synthesized following procedures described earlier [21]. 4-*n*-Alkylbiphenyl-4-carboxylic acids were synthesized following a procedure described previously [22, 23]. A detailed procedure for one of the target compounds and its physical data are given below.

**2.2.1. 5-Chlororesorcinol, b.** A solution of 1-chloro-3,5-dimethoxybenzene **a** (5.0 g, 28.94 mmol) in dry dichloromethane (50 ml) was cooled to −78°C. A solution of boron tribromide (28.98 g, 115.76 mmol) in dichloromethane (20 ml) was added to this solution dropwise over a period of 2 h. The temperature was maintained for 2–3 h, then allowed slowly to fall to room temperature. The reaction mixture was then stirred for about 10 h at room temperature and heated at reflux for a further 10 h. Excess of boron tribromide was decomposed carefully by the addition of moist chloroform; a dark product obtained on removal of solvent was passed through a column of silica gel using 5% ethyl acetate in chloroform as eluant. The product thus obtained was further purified by short path distillation; yield 3.5 g (83.5%), m.p. 115–116°C. IR (Nujol) $\nu_{\max}$: 3622, 3261, 2923, 2854, 2692, 2489, 1604, 1469, 1093 $\mathrm{cm}^{-1}$. $^1$H NMR ($CDCl_3$, 400 MHz) $\delta$: 8.0 (s, 2H, 2 × Ar–OH, exchangeable with $D_2O$), 6.64–6.60 (t, 1H, $^4J$=2 Hz, Ar–H), 6.20–6.10 (m, 2H, Ar–H). Elemental analysis: $C_7H_5O_2Cl$ requires C 49.85, H 3.48; found C 49.55 H 3.4%.

**2.2.2. 5-Chloro-1, 3-phenylene bis(3-fluoro-4-benzyloxybenzoate), c (X=H, Y=F).** A mixture of 5-chlororesorcinol (1 g, 6.9 mmol), 3-fluoro-4-benzyloxybenzoic acid (3.4 g, 13.8 mmol), and a catalytic amount of 4-(*N*,*N*-dimethylamino) pyridine (DMAP) in dry dichloromethane (25 ml) was stirred for 10 min. To this mixture, *N*,*N′*-dicyclohexylcarbodiimide (DCC) (3.08 g, 15.18 mmol) was added and stirred for about 12 h at room temperature. The precipitated *N*,*N′*-dicyclohexylurea was filtered off and washed with an excess of dichloromethane. The combined organic solution was washed with ice-cold aqueous 5% sodium hydroxide solution (2 × 50 ml), 5% aqueous acetic acid (2 × 50 ml) and finally with water (3 × 60 ml) and dried over sodium sulphate. The residue obtained on removal of solvent was chromatographed on silica gel using chloroform as eluant. The material obtained on removal of the solvent was further purified by crystallization using acetonitrile; yield 3 g (75%), m.p. 126–127°C. IR (Nujol) $\nu_{\max}$: 2923, 2854, 2669, 1743, 1735, 1733, 1730, 1460 $\mathrm{cm}^{-1}$. $^1$H NMR ($CDCl_3$, 400 MHz) $\delta$: 8.07–8.03 (t, 2H, $^3J$=8.64 Hz, Ar–H), 7.45–7.39 (m, 10H, Ar–H), 7.22 (d, 2H, $^4J$=2 Hz, Ar–H), 7.14–7.13 (t, 1H, $^4J$=2 Hz, Ar–H), 6.90–6.87 (dd, 2H, $^3J$=8.8 Hz, $^4J$=2.3 Hz, Ar–H), 6.82–6.78 (dd, 2H, $^3J$=12.6 Hz, $^4J$=2.4 Hz, Ar–H), 5.16 (s, 4H, 2 × $ArCH_2O$–).

**2.2.3. 5-Chloro-1, 3-phenylene bis(3-fluoro-4-hydroxybenzoate), d (X=H, Y=F).** Compound **c** (3 g) was dissolved in 1,4-dioxane (50 ml) and 5% Pd-C catalyst

(0.6 g) added. The mixture was stirred at 60°C in an atmosphere of hydrogen until the required quantity of hydrogen was absorbed. The resulting mixture was filtered hot and the solvent removed under reduced pressure. The material so obtained was crystallized using a mixture of butan-2-one and petroleum ether (b.p.60–80°C); yield 2.0 g (87.7%), m.p. 220–221°C. IR (Nujol) $\nu_{\max}$: 3371, 2954, 2923, 2854, 1720, 1706, 1616 $\mathrm{cm}^{-1}$. $^1$H NMR ($CDCl_3$, 400 MHz) $\delta$: 11.09(s, 2H, $2\times$Ar–OH, exchangeable with $D_2O$), 7.99–7.94 (t, 2H, $^3J$=8.76 Hz, Ar–H), 7.45–7.44 (d, 2H, $^4J$=2 Hz, Ar–H), 7.31–7.30 (t, 1H, $^4J$=2 Hz, Ar–H), 6.81–6.78 (dd, 2H, $^3J$=8.72 Hz, $^4J$=2.16 Hz, Ar–H), 6.75–6.72 (dd, 2H, $^3J$=13.04 Hz, $^4J$=2.12 Hz, Ar–H).

**2.2.4. 5-Chloro-1,3-phenylene bis[4-(4-n-octadecylbiphenyl-4′-carbonyloxy)-3-fluoro benzoate)], 22 (X=H, Y=F, n=18).** A mixture of compound **d** (0.1 g, 0.23 mmol), 4-*n*-octadecylbiphenyl-4-carboxylic acid (0.214 g 0.46 mmol) and a catalytic amount of DMAP in dry dichloromethane (8 ml) was stirred for 10 min. To this stirred mixture, DCC (0.107 g, 0.52 mmol) was added and the stirring continued for about 12 h. The solvent was removed and the residue purified by column chromatography on silica gel using chloroform as eluant. The product thus obtained was purified further by repeated crystallization from butan-2-one; yield 0.12 g (39%), m.p. 135°C. IR (KBr) $\nu_{\max}$: 2918, 2848, 1735, 1739, 1745, 1598 $\mathrm{cm}^{-1}$. $^1$H NMR ($CDCl_3$, 400 MHz) $\delta$: 8.29–8.27 (d, 4H, $^3J$=8.48 Hz, Ar–H), 8.24–8.20 (dd, 2H, $^4J$=8.52 Hz, Ar–H), 7.79–7.77 (d, 4H, $^3J$=8.48 Hz, Ar–H), 7.63–7.61 (d, 4H, $^3J$=8.12 Hz, Ar–H), 7.30–7.25 (m, 6H, Ar–H), 7.23–7.22 (t, 1H, $^4J$=2.04 Hz, Ar–H), 2.72–2.68 (t, 4H, $^3J$=7.48 Hz, $2\times$Ar–$CH_2$–), 1.71–1.66 (quin, 4H, $^3J$=6.56 Hz, $2\times$Ar–$CH_2$–$\underline{CH_2}$–), 1.37–1.29 (m, 60H, $30\times$–$CH_2$–), 0.93–0.89 (t, 6H, $^3J$=6.56 Hz, $2\times$–$CH_2$–$\underline{CH_3}$). $\delta_C$: 163.6, 162.8, 153.0, 151.5, 147.0, 143.7, 137.0, 131.0, 129.2, 127.8, 127.2, 126.9, 126.5, 124.5, 120.2, 118.9, 118.7, 114.3, 35.7, 32.0, 31.5, 29.7, 29.5, 29.4, 22.7, 14.1. Elemental analysis: $C_{79}H_{99}ClF_2O_8$ requires C 75.9, H 7.9; found C 76.08, H 7.79%.

## 3. Results and discussion

### 3.1. *Microscopic observations*

The transition temperatures and associated enthalpy values for the two series of compounds, I and II, are summarized in tables 1 and 2, respectively. The two series of compounds differ from one another by the position of the fluorine substituent in the side arms of the bent-core molecules. It can be seen in table 1 that compound **1** is dimorphic. The higher temperature phase exhibits a focal-conic texture, and when viewed between two glass plates treated for homeotropic alignment of the sample, remains birefringent. Even after shearing the mesophase, it remains birefringent and this has been characterized as an intercalated smectic ($B_6$) phase. The enthalpy value of isotropization is 19.9 kJ $\mathrm{mol}^{-1}$, and the thermal range of this mesophase is 18°C. On cooling the mesophase, a transition takes place at 195°C with a low enthalpy of 0.34 kJ $\mathrm{mol}^{-1}$, and a small change in the texture occurs. There was no significant change in the texture of the mesophase on lowering the temperature further; however, on shearing the sample, one could clearly see a mosaic texture that is normally seen for a classical $B_1$ phase. The mesophases of compounds **2**, **3** and **4** also exhibit this mosaic texture and, except for the mesophase of compound **4** which is metastable, are enantiotropic. This mesophase has been identified as a rectangular columnar $B_1$ phase using XRD studies (see later) and it does not switch electro-optically. Surprisingly compounds **5**–**8** show no mesophase behaviour even on fast cooling of their isotropic phases. However, compounds **9**–**11** show a mesophase with similar optical textures. Although compound **9** shows a metastable phase, the clearing enthalpy values for all three compounds are quite similar. The optical textures show features reminiscent of those seen for the $B_{2x}$ mesophase exhibited by compounds derived from 5-cyanoresorcinol [19]. Specifically, fingerprint and schlieren textures, patterns showing single-wound helix and filaments were obtained.

Unlike the compounds of series I, all the homologues of series II are enantiotropic liquid crystals. Compounds **12**–**19** exhibit the typical mosaic texture seen for the $B_1$ phase and XRD data clearly showed that the mesophase has a rectangular lattice. Hence, we have designated the mesophase of all these compounds as $B_1$. It is interesting to note that compound **12** has a thermal range of 48.5°C for the $B_1$ phase; this range gradually decreases and is only 16°C for compound **19**. Again, as mentioned earlier, this phase does not respond to an externally applied electric field. The remaining three compounds **20**–**22** are lamellar as indicated by XRD studies, and show unusual optical textures. For example, when the isotropic liquid of compound **22** was cooled slowly, filamentary growth patterns could be seen; a photomicrograph of a typical growing filament is shown in figure 1. Normally the mesophase exhibited a helical pattern, including single and doubly-wound helices and filaments; a typical pattern obtained is shown in figure 2. As the temperature is lowered, the filaments transform to a helical pattern and finally both collapse to form an undefined structure (fringe pattern),

Table 1. Transition temperatures (°C) and associated enthalpies (kJ mol$^{-1}$, *in italics*) for compounds of series I. Cr=crystalline phase; $B_{2x}$=variant of a $B_2$ phase; $B_1$=columnar phase with a rectangular lattice; I=isotropic phase.

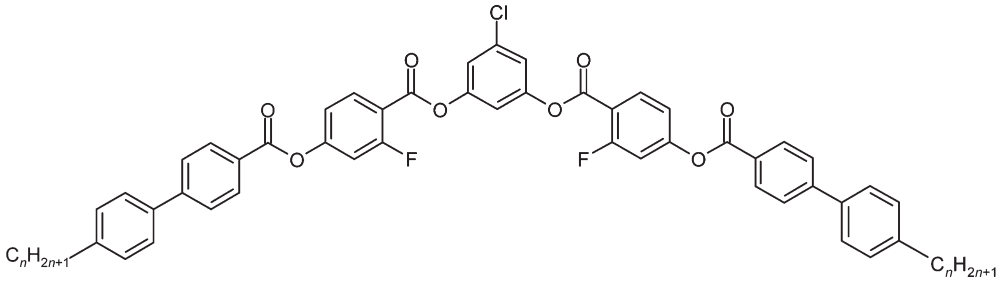

| Compound | $n$ | Cr | | $B_{2x}$ | | $B_1$ | | $B_6$ | | I |
|---|---|---|---|---|---|---|---|---|---|---|
| **1** | 5 | • | 182.5<br>*46.2* | — | | • | 195.0<br>*0.34* | • | 213.0<br>*19.9* | • |
| **2** | 6 | • | 188.0<br>*31.2* | — | | • | 198.5<br>*21.7* | — | | • |
| **3** | 7 | • | 180.0<br>*28.3* | — | | • | 192.0<br>*23.6* | — | | • |
| **4** | 8 | • | 184.0<br>*55.1* | — | | (• | 179.5)<br>*22.8* | — | | • |
| **5** | 9 | • | 183.5<br>*55.2* | — | | — | | — | | • |
| **6** | 10 | • | 180.5<br>*55.1* | — | | — | | — | | • |
| **7** | 11 | • | 179.0<br>*54.3* | — | | — | | — | | • |
| **8** | 12 | • | 174.5<br>*63.2* | — | | — | | — | | • |
| **9** | 14 | • | 170.5<br>*53.8* | (• | 164.0)<br>*23.4* | — | | — | | • |
| **10** | 16 | • | 157.5<br>*21.1* | • | 167.0<br>*24.1* | — | | — | | • |
| **11** | 18 | • | 157.0<br>*23.9* | • | 167.5<br>*24.0* | — | | — | | • |

but some areas do show schlieren texture. These features are not observed in the $B_2$ phase and, coupled with electro-optical investigations (see later), the mesophase of the three compounds **9**–**11** and compounds **20**–**22** have been designated as $B_{2x}$. Plots of the transition temperature as a function of the length of the terminal $n$-alkyl chain for series I and II compounds are shown in figures 3 and 4, respectively. A comparison of these plots, clearly reveals that $m$-fluorine-substituted compounds (series II) are more conducive to generating mesophases. Moreover, both the melting and clearing temperatures are lower for these compounds.

### 3.2. *X-ray diffraction studies*

In order to determine the structure of the mesophases under investigation, XRD studies were carried out on a number of representative compounds. The compounds were placed in 0.5 mm Lindemann capillaries and cooled slowly from their isotropic phases. The XRD data obtained for the unoriented mesophases of eight compounds are summarized in table 3. The XRD pattern of an unoriented sample of compound **19** showed three reflections in the small angle region with $d_1$=37.45, $d_2$=26.56, and $d_3$=16.59 Å. These could be indexed as reflections from (1 1), (0 2) and (3 1) planes, formed by a rectangular lattice with lattice parameters $a$=52.8 and $b$=53.12 Å. The X-ray diffractogram obtained for the mesophase of this compound is shown in figure 5. The XRD pattern obtained for the mesophase of compound **22** showed two reflections in the small angle region at $d_1$=50.8 and $d_2$=25.4 Å. These reflections are in the ratio 1:1/2 indicating a lamellar ordering of the molecules in the mesophase. The first

Table 2. Transition temperatures (°C) and associated enthalpies (kJ mol$^{-1}$, *in italics*) for the compounds of series II. Cr=crystalline phase; $B_{2x}$=variant of a $B_2$ phase; $B_1$=columnar phase with a rectangular lattice; I=isotropic phase.

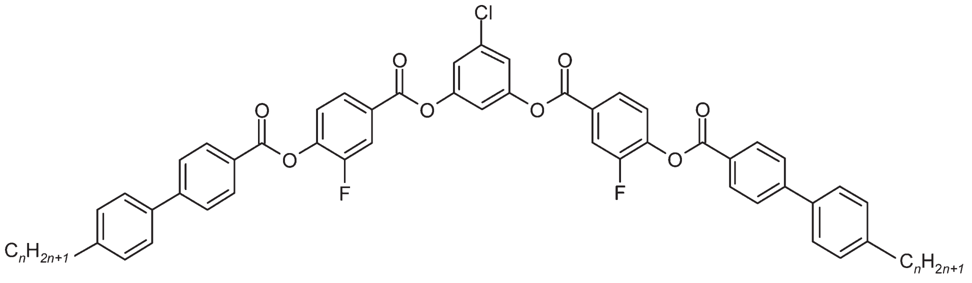

| Compound | $n$ | Cr | | $B_{2x}$ | | $B_1$ | | I |
|---|---|---|---|---|---|---|---|---|
| **12** | 5 | • | 161.0 | — | | • | 209.5 | • |
| | | | *31.7* | | | | *18.5* | |
| **13** | 6 | • | 144.5 | — | | • | 199.0 | • |
| | | | *32.4* | | | | *20.0* | |
| **14** | 7 | • | 155.0 | — | | • | 193.5 | • |
| | | | *56.5* | | | | *21.7* | |
| **15** | 8 | • | 155.0 | — | | • | 186.5 | • |
| | | | *56.5* | | | | *22.6* | |
| **16** | 9 | • | 158.5 | — | | • | 181.5 | • |
| | | | *59.5* | | | | *23.2* | |
| **17** | 10 | • | 137.5 | — | | • | 173.5 | • |
| | | | *21.9* | | | | *23.5* | |
| **18** | 11 | • | 141.0 | — | | • | 167.5 | • |
| | | | *22.6* | | | | *22.6* | |
| **19** | 12 | • | 144.5 | — | | • | 160.5 | • |
| | | | *23.2* | | | | *20.8* | |
| **20** | 14 | • | 136.5 | • | 154.5 | — | | • |
| | | | *23.3* | | *20.5* | | | |
| **21** | 16 | • | 135.5 | • | 154.5 | — | | • |
| | | | *23.6* | | *20.3* | | | |
| **22** | 18 | • | 135.0 | • | 154.0 | — | | • |
| | | | *20.8* | | *20.3* | | | |

Figure 1. Photomicrograph of a filament growing on cooling the isotropic phase of compound **22** at 153.8°C; magnification ×200.

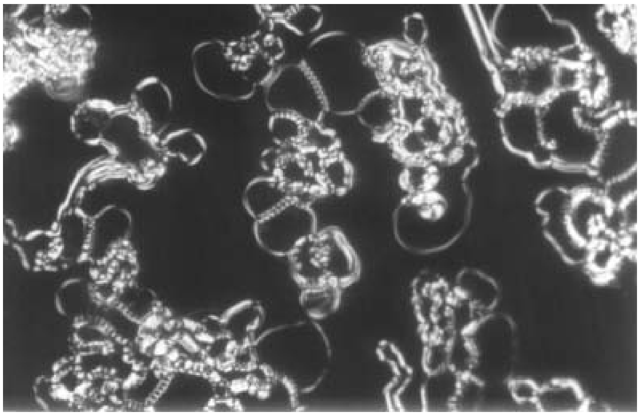

Figure 2. Photomicrograph of the texture obtained on cooling slowly the isotropic phase of compound **22** in a polyimide-coated cell of thickness 6.5 μm at 151°C; magnification ×200.

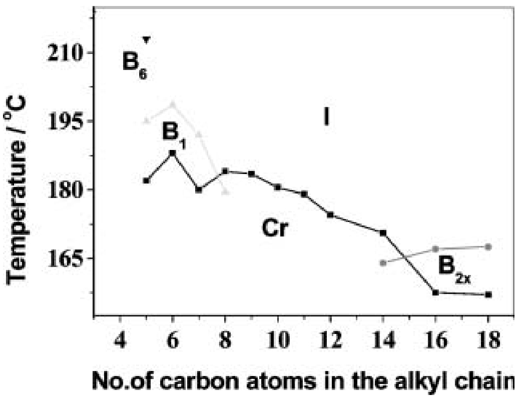

Figure 3. Plot of transition temperatures vs the number of carbon atoms in the *n*-alkyl chain for compounds of series I.

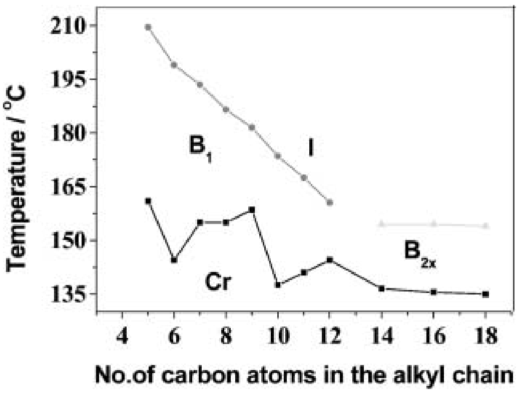

Figure 4. Plot of transition temperatures vs the number of carbon atoms in the *n*-alkyl chain for compounds of series II.

order layer spacing is smaller than the measured molecular length, assuming the terminal chains to be in an all-*trans*-conformation. This suggests a tilt angle of 53°–55° for the molecules with respect to the layer normal. In the wide angle region a diffuse maximum at about 4.6 Å was obtained which indicates the absence of in-plane order. The X-ray diffractogram obtained for the mesophase of this compound **22** is shown in figure 6.

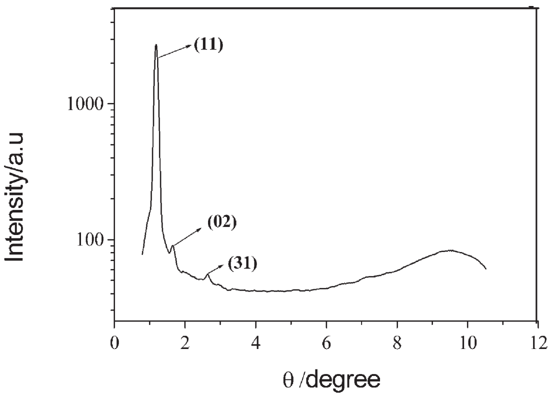

Figure 5. X-ray angular intensity profile obtained for the $B_1$ mesophase of compound **19**.

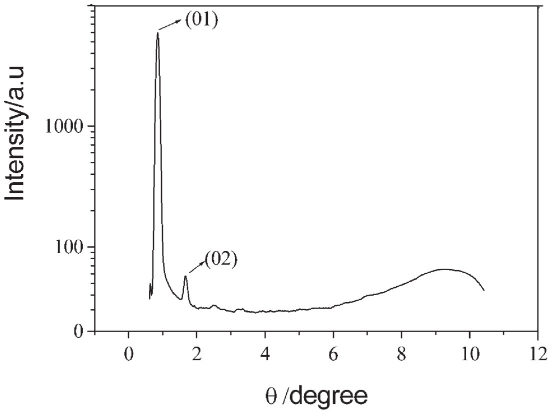

Figure 6. X-ray angular intensity profile obtained for the $B_{2x}$ mesophase of compound **22**.

### 3.3. *Electro-optical investigations*

Electro-optical investigations were carried out on the $B_{2x}$ mesophase exhibited by compounds belonging to both series. Since the characteristic behaviour was the same, only the experimental observations made on compound **22** are described in detail. For the a.c. field experiments, a sample of compound **22** in its isotropic

Table 3. Spacings (Å) obtained for the mesophases of different compounds; the corresponding Miller indices are given in brackets.

| Compound | *d*-spacings/Å(Miller indices) | Lattice parameters/Å | | Phase type | *T*/°C |
|---|---|---|---|---|---|
| | | a | b | | |
| **3** | 24.75 (1 1), 22.16 (0 2) | 29.83 | 44.33 | $B_1$ | 170 |
| **9** | 42.8 (0 1), 21.4 (0 2) | — | — | $B_{2x}$ | 162 |
| **10** | 44.27 (0 1), 22.44 (0 2) | — | — | $B_{2x}$ | 162 |
| **11** | 46.8 (0 1), 23.43 (0 2) | — | — | $B_{2x}$ | 162 |
| **15** | 29.8 (1 1), 24.7 (0 2) | 37.38 | 49.4 | $B_1$ | 165 |
| **16** | 32.69 (1 1), 25.02 (0 2) | 43.11 | 50.14 | $B_1$ | 165 |
| **19** | 37.45 (1 1), 26.56 (0 2), 16.59 (3 1) | 52.8 | 53.12 | $B_1$ | 150 |
| **22** | 50.8 (0 1), 25.4 (0 2) | — | — | $B_{2x}$ | 145 |

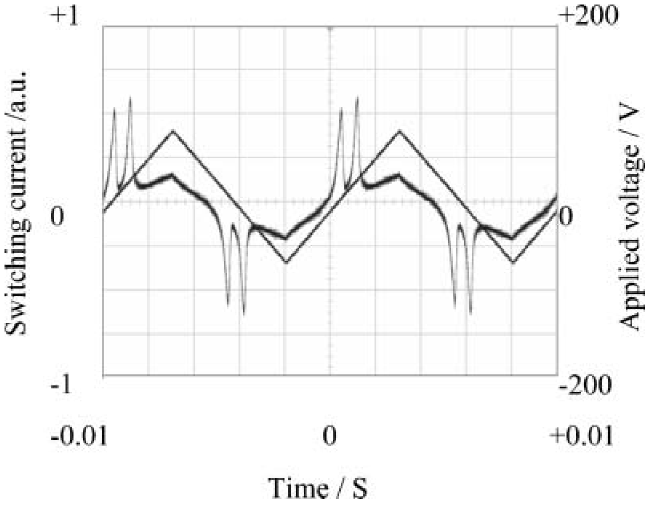

Figure 7. Switching current response obtained for the mesophase of compound **22** by applying a triangular wave voltage (150 $V_{pp}$, 10 Hz), cell thickness 11.5 μm, temperature 145°C; saturated polarization value 710 nC cm$^{-2}$.

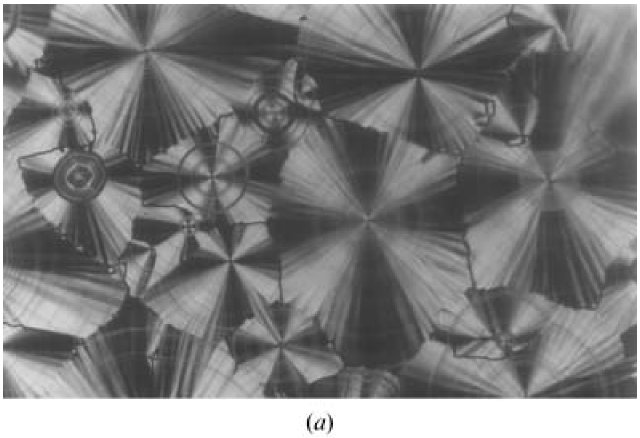
(*a*)

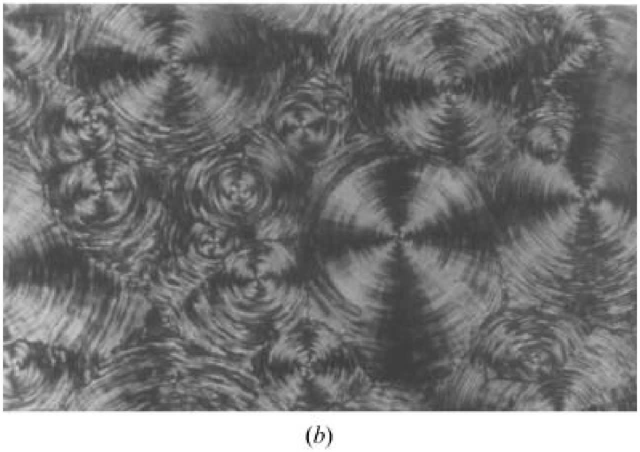
(*b*)

Figure 8. Photomicrographs showing the optics of the mesophase of compound **22** on the application of a triangular wave voltage of (*a*) 150 $V_{pp}$, 10 Hz and (*b*) 0 V, at 145°C.

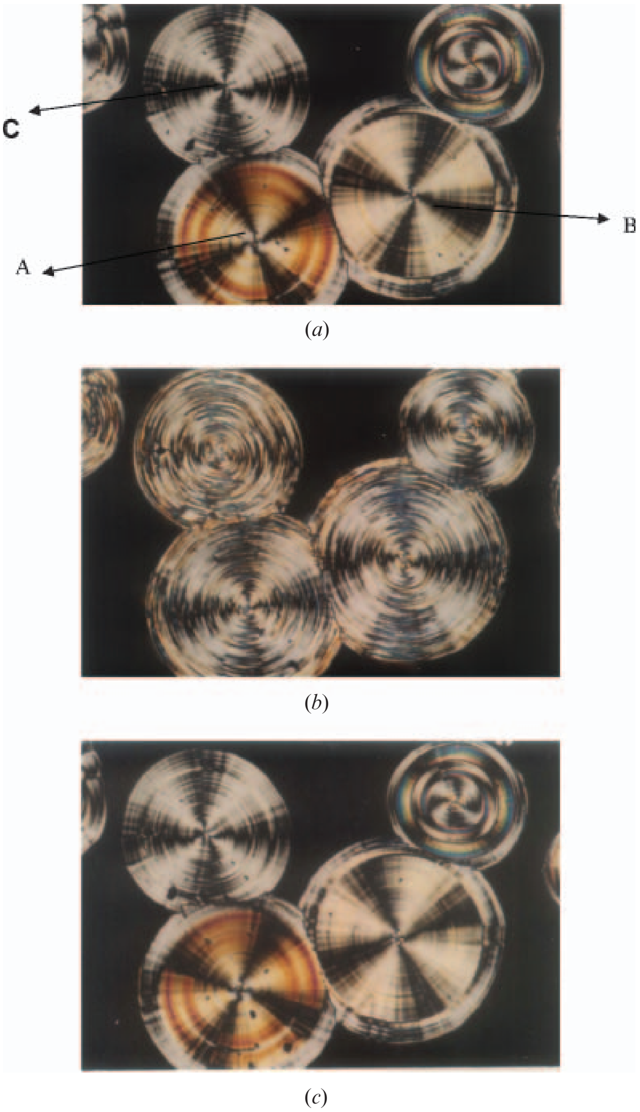

(*a*)

(*b*)

(*c*)

Figure 9. Photomicrographs obtained for the $B_{2x}$ phase of compound **22** by the application of a d.c. electric field of (*a*) +2 V μm$^{-1}$, (*b*) 0 V and (*c*) −2 V μm$^{-1}$.

phase was filled into an ITO-coated home-made cell of uniform thickness 11.5 μm, which was treated for homogeneous alignment. The sample was cooled slowly from the isotropic phase under a triangular wave voltage of 40 $V_{pp}$ and a frequency of 10 Hz, while simultaneously the optical behaviour was observed under a polarizing light microscope. Two polarization current peaks per half cycle were observed at a very low threshold voltage of 60 $V_{pp}$ and a frequency of 10 Hz, indicating an antiferroelectric ground state for the mesophase. Circular domains were seen under the microscope in which the extinction cross coincides with the direction of the crossed polarizer and analyser, indicating an anticlinic arrangement of the molecules.

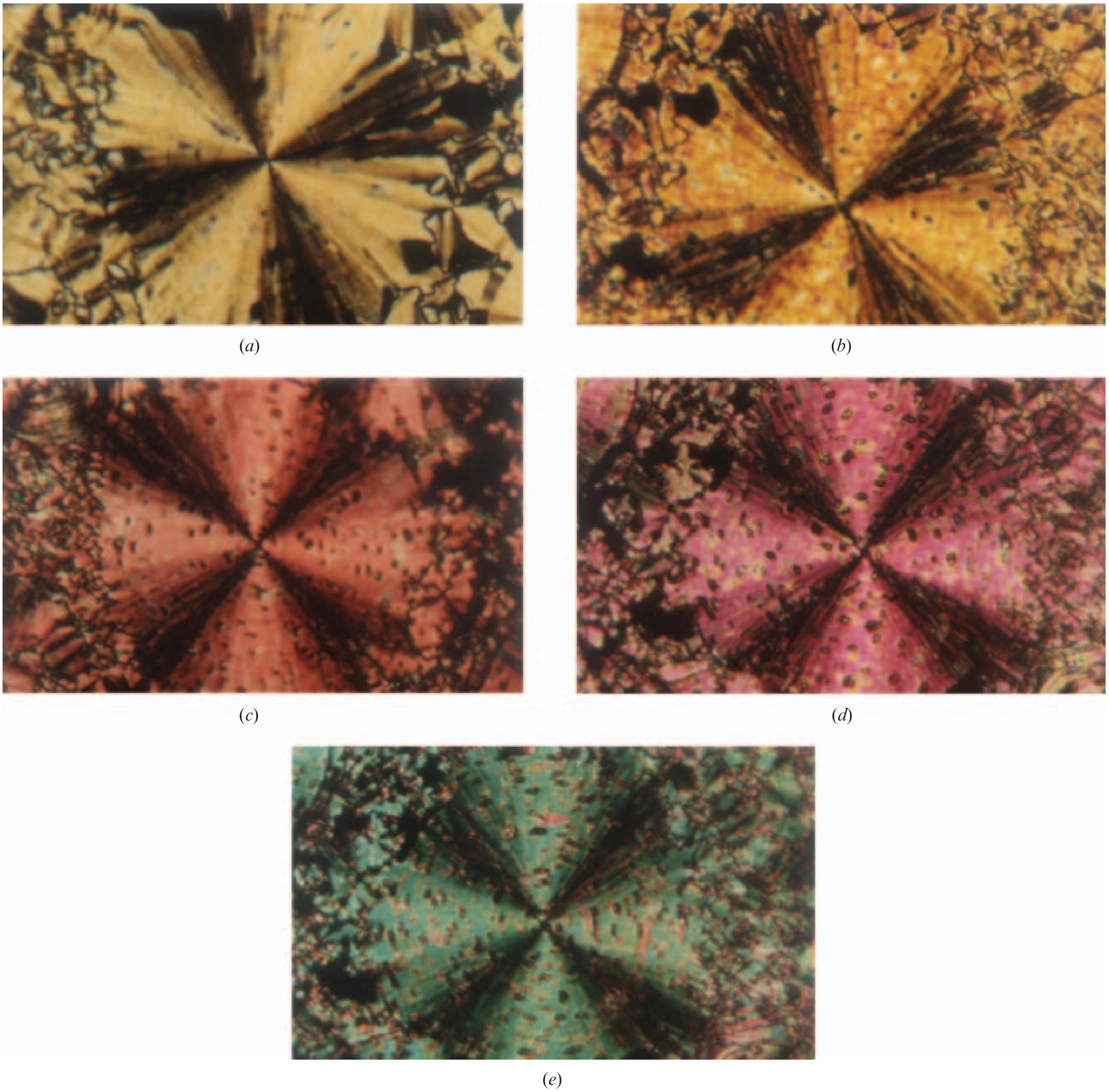

Figure 10. Photomicrographs illustrating the variation of colour and rotation of extinction crosses with the variation of the d.c. field for the mesophase of compound **22**: (*a*) 1, (*b*) 1.5, (*c*) 2.0, (*d*) 2.5, (*e*) 3.0 $\mathrm{V\,\mu m^{-1}}$.

Even after switching off the field, the orientation of the cross did not change. This is possibly due to the molecules relaxing to the ground state through a rotation around their long molecular axis, in which case there is no change in the tilt direction. The switching current response obtained in the $B_{2x}$ phase of compound **22** at 145°C is shown in figure 7 and the corresponding optical photomicrographs obtained with $E=150\,\mathrm{V_{pp}}$ at 10 Hz and $E=0\,\mathrm{V}$ are shown in figure 8. The calculated average saturated polarization value is about $710\,\mathrm{nC\,cm^{-2}}$.

The mesophase of compound **22** was also examined under a d.c. electric field, using a cell of thickness 9.9 μm. On slow cooling of the isotropic phase of this compound under a d.c. field of $1.5\,\mathrm{V\,\mu m^{-1}}$, various circular domains were obtained. However, the observations were made slightly above this threshold voltage. For example, as shown in figure 9 with a field of

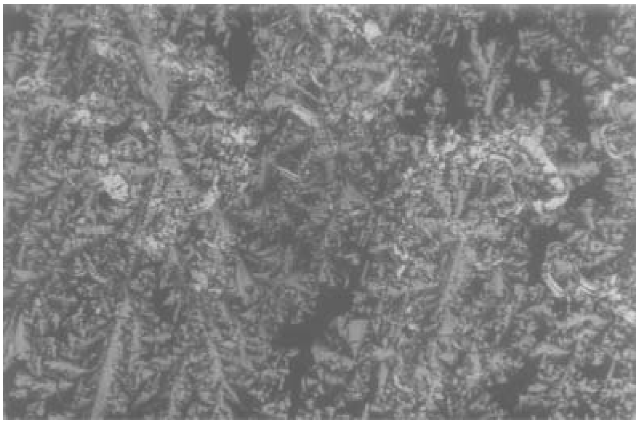

Figure 11. Photomicrograph showing the field-induced growth of the mesophase of compound **22** at a d.c. electric field of 57 V; temperature 155°C; cell thickness 6.78 μm.

$+2\,\mathrm{V\,\mu m^{-1}}$, two domains (A and B) were observed in which the extinction crosses rotate in clock-wise and counter clock-wise directions, respectively, with respect to the polarizer and analyser. On reversing the polarity of the applied field, the extinctions which rotated in a clock-wise direction now rotate in an anticlock-wise direction and *vice versa*. On terminating the field, the extinction crosses in these domains orient parallel to the axes of the crossed polarizers. This clearly indicates a synclinic ferroelectric state under the field, which relaxes to the anticlinic antiferroelectric ground state, thus representing the two ferroelectric conglomerates. In domain C, the extinction cross lies parallel to the polarizer and analyser with the field, and no change of this orientation was observed either on reversing the polarity of the field or on switching off the field. However, smooth circular domains obtained with the field were replaced by stripes appearing on the fans when the field was switched off. These observations are in accord with the layer structure model proposed [2], in which the molecules in adjacent layers have a synclinic tilt and a change in the tilt direction takes place after a few layers. The stripes on the domains indicate the region where there is a change in the tilt; similar observations have previously been made [19, 24]. A schematic representation of the arrangement of molecules in adjacent layers in each domain, that are responsible for the occurrence of heterochiral domains, has been given earlier [6, 19].

It is interesting to note the variation of colour as a function of the strength of the applied d.c. field. For example, on increasing the strength of the field, the colour changes from yellow to green and the extinction brush rotates linearly with the field; this process is reversible (see figure 10). All these observations are quite similar to those obtained for the $B_{2x}$ mesophase exhibited by compounds derived from 5-cyanoresorcinol [19].

Another interesting feature is the growth of the mesophase above the clearing temperature when a sufficiently high d.c. field is applied. For compound **22** at 155°C, when a d.c. field of 43 V was applied, the mesophase started to nucleate and covered the whole field of view on enhancing the strength of the applied field (57 V). A photomicrograph of this field-induced growth of the mesophase is shown in figure 11. On increasing the temperature further, the field required to induce the nucleation also increased. This type of observation has been made previously [25, 26] and indicates the existence of short range orientational order of the molecules in the isotropic phase.

## 4. Summary and conclusions

The synthesis and characterization of two new homologous series of seven-ring bent-core esters derived from 5-chlororesorcinol have been carried out. These represent the first example of BC compounds containing a chloro substituent at position-5 of the central phenyl unit. The lower homologues of both series of compounds exhibit the rectangular columnar $B_1$ phase. Interestingly, the higher homologues show a mixture of three different possible structures, two chiral and one racemic. Since the $B_{2x}$ mesophase shows a helical pattern similar to that observed in [6], and we were unable to carry out high resolution XRD, it is possible that this mesophase is among the $B_7$ class of materials.

## Acknowledgements

The authors thank Ms K. N. Vasudha for technical support, Mr N. Balakrishnaprabhu for help in XRD measurements, and the Sophisticated Instruments Facility, Indian Institute of Science, Bangalore, for recording the NMR spectra.

## References

[1] T. Niori, T. Sekine, J. Watanabe, T. Furukawa, H. Takezoe. *J. mater. Chem.*, **6**, 1231 (1996).

[2] D.R. Link, G. Natale, R. Shao, J.E. MacLennan, E. Körblova, N.A. Clark, D.M. Walba. *Science*, **278**, 1924 (1997).

[3] G. Pelzl, S. Diele, W. Weissflog. *Adv. Mater.*, **11**, 707 (1999).

[4] B.K. Sadashiva, V.A. Raghunathan, R. Pratibha. *Ferroelectrics*, **243**, 249 (2000).

[5] R. Amaranatha Reddy, B.K. Sadashiva. *Liq. Cryst.*, **30**, 1031 (2003).

[6] D.M. Walba, E. Körblova, R. Shao, J.E. MacLennan, D.R. Link, M.A. Glaser, N.A. Clark. *Science*, **288**, 2181 (2000).

[7] J.P. Bedel, J.C. Rouillon, J.P. Marcerou, M. Laguerre, H.T. Nguyen, M.F. Achard. *Liq. Cryst.*, **27**, 1411 (2000).

[8] H. Nadasi, W. Weissflog, A. Eremin, G. Pelzl, S. Diele, B. Das, S. Grande. *J. mater. Chem.*, **12**, 1316 (2002).

[9] R. Amaranatha Reddy, B.K. Sadashiva. *J. mater. Chem.*, **12**, 2627 (2002).

[10] C. Tschierske, G. Dantlgraber. *Pramana*, **61**, 455 (2003).

[11] R. Amaranatha Reddy, B.K. Sadashiva. *Liq. Cryst.*, **29**, 1365 (2002).

[12] R. Amaranatha Reddy, B.K. Sadashiva. *Liq. Cryst.*, **30**, 273 (2003).

[13] H.N. Shreenivasa Murthy, B.K. Sadashiva. *Liq. Cryst.*, **30**, 1051 (2003).

[14] H.N. Shreenivasa Murthy, B.K. Sadashiva. *J. mater. Chem.*, **13**, 2863 (2003).

[15] G. Heppke, D.D. Parghi, H. Sawade. *Ferroelectrics*, **243**, 269 (2000).

[16] G. Heppke, D.D. Parghi, H. Sawade. *Liq. Cryst.*, **27**, 313 (2000).

[17] C.K. Lee, A. Primak, A. Jakli, E.J. Cho, W.C. Zin, L.-C. Chien. *Liq. Cryst.*, **28**, 1293 (2001).

[18] D.A. Coleman, J. Fernsler, N. Chattham, M. Nakata, M. Takanishi, E. Körblova, D.R. Link, R.-F. Shao, W.G. Jang, J.E. MacLennan, O. Mondainn-Monval, C. Boyer, W. Weissflog, G. Pelzl, L.-C. Chien, J. Zasadzinski, J. Watanabe, D.M. Walba, H. Takezoe, N.A. Clark. *Science*, **301**, 1204 (2003).

[19] R. Amaranatha Reddy, B.K. Sadashiva. *Liq. Cryst.*, **31**, 1069 (2004).

[20] G.W. Gray, C. Hogg, D. Lacey. *Mol. Cryst. liq. Cryst.*, **67**, 1 (1981).

[21] N. Kasthuraiah, B.K. Sadashiva, S. Krishnaprasad, G.G. Nair. *Liq. Cryst.*, **24**, 639 (1998).

[22] D. Coates, G.W. Gray. *Mol. Cryst. liq. Cryst.*, **37**, 249 (1976).

[23] B.K. Sadashiva, G.S.R. Subba Rao. *Mol. Cryst. liq. Cryst.*, **38**, 703 (1977).

[24] M. Zennyoji, Y. Takanishi, K. Ishikawa, J. Thisayukta, J. Watanabe, H. Takezoe. *J. mater. Chem.*, **9**, 2775 (1999).

[25] W. Weissflog, M.W. Schröder, S. Diele, G. Pelzl. *Adv. Mater.*, **15**, 630 (2003).

[26] M.W. Schröder, G. Pelzl, U. Dunemann, W. Weissflog. *Liq. Cryst.*, **31**, 633 (2004).